THE PROGRAM FANS-3D (FINITE ANALYTIC NUMERICAL SIMULATION 3-DIMENSIONAL) AND ITS APPLICATIONS

Ramiro H. Bravo[1]
Tri-State University
Angola, Indiana 46703

Ching-Jen Chen[2]
University of Iowa
Iowa City, Iowa 52242

SUMMARY

In this study, the program named FANS-3D (Finite Analytic Numerical Simulation - 3 Dimensional) is presented. FANS-3D was designed to solve problems of incompressible fluid flows and combined modes of heat transfer. It solves problems with conduction and convection modes of heat transfer in laminar flow, with provisions for radiation and turbulent flows. It can solve singular or conjugate modes of heat transfer. It also solves problems in natural convection, using the Boussinesq approximation. FANS-3D was designed to solve heat transfer problems inside one, two and three dimensional geometries that can be represented by orthogonal planes in a Cartesian coordinate system. It can solve internal and external flows using appropriate boundary conditions such as symmetric, periodic and user specified.

INTRODUCTION

The program FANS-3D solves one, two and three dimensional fluid flow and heat transfer problems that involve conduction and convection modes of heat transfer in incompressible laminar flow, with provisions for radiative heat transfer and buoyant and turbulent flows. It also solves problems in natural convection using the Boussinesq approximation. Using this feature, the program may also solve mixed natural and forced convection problems. Furthermore, it can solve individual modes of heat transfer as well. The program FANS-3D solves any geometry that can be represented by orthogonal planes in a Cartesian coordinate system. The program can solve internal and external flows using appropriate boundary conditions such as symmetric, periodic and user specified. The program is designed to have the same performance in all directions, in this way, any problem can be solved in the most convenient orientation.

The program FANS-3D is based on the 19-point Finite Analytic Method. It uses the SIMPLEC iterative method suggested by Van Doormal and Raithby (1984) to solve the coupled Navier-Stokes equations. The discretization of variables is done following a new staggered grid layout. The resulting system of algebraic equations is solved by different methods, including ADI, SSOR and Conjugate Gradient.

The program has two modules; a graphics and a computational. The graphics module, named GRAPH3D, was written in FORTRAN 77 for Apollo workstations. This program displays the geometry of solution and the results in the three-dimensional space. These are

---

1 Assistant Professor Department of Aerospace and Mechanical Engineering.
2 Professor and Chairman Department of Mechanical Engineering.

presented in the form of velocity vectors, profiles, and color contours with shading of any variable. These graphic results can also be sent to monochrome and color printers.

The computational module of the program is divided in two parts. The first, which is accessible to the user, should be modified according to the problem. The second part is fixed and does not require user intervention. These two parts must be bound together to create the computational 'run' file. Both parts of the computational module are written in standard FORTRAN 77 language. In this form the program can be easily ported to almost any machine.

THE STRUCTURE OF THE PROGRAM FANS-3D

As mentioned above, the program FANS-3D is based on the 19 Point Finite Analytic Method. The basic idea of this method is illustrated here. Details of its derivation are given by Bravo et. al. (1991). This method is derive for the general transport equation

$$\phi_{xx} + \phi_{yy} + \phi_{zz} = D\,\phi_t + 2A\,\phi_x + 2B\,\phi_y + 2C\,\phi_z - S\,h \qquad (1)$$

using the analytic solutions of simplified forms of it. To start, this equation is first locally linearized in the three-dimensional element shown in figure 1. To this effect, the coefficients A, B, C, D and the source term S are assumed constants and equal to their values at the center of the element, i.e.

$$\phi_{xx} + \phi_{yy} + \phi_{zz} = D_p\phi_t + 2A_p\phi_x + 2B_p\phi_y + 2C_p\phi_z - S_p \qquad (2)$$

The p subindices mean that these coefficients are considered constant inside the element and equal to their values at the center 'p'. For example, if ϕ is the u velocity component in a laminar flow and R the Reynolds number, then $A_p = Ru_p/2$, $B_p = Rv_p/2$, $C_p = Rw_p/2$, $D = R$ and $S_p = -RP_x$. Equation (2) is then solved in the planes x=0, y=0 and z=0 and shown in figure 2. These two-dimensional solutions are combined to obtain the three-dimensional 19-point finite analytic scheme. Details of this process are given by Bravo et. al. (1991).

The solution of the coupled Navier-Stokes equations present an additional inconvenience; there is no clear equation for pressure. To solve this problem many methods have been developed. Notable examples are SIMPLE (Semi-Implicit Method for Pressure Linked Equations) of Patankar and Spalding (1972), SIMPLER (Patankar, 1980), SIMPLEC (Van Doormal and Raithby, 1984) and PISO (Issa et. al., 1986). Most of these methods are generally known as pressure correction methods. The program FANS-3D uses the SIMPLER and SIMPLEC methods. The discretized system of equations when used with the Finite Analytic Method can be found in the works of Bravo (1987) and Aksoy (1989).

Another major difficulty in the implementation of the numerical schemes to incompressible fluid flow problems is the choice of a proper computational grid. Clearly, it would be beneficial if one could discretize the governing equation using a grid system that places all the flow variables, scalar and vector, at the same physical location. Unfortunately, the use of such a nonstaggered grid system with a primitive variable formulation of the incompressible equations has been shown to produce nonphysical oscillations in the pressure field (Patankar, 1980). A remedy to this problem is the use of a staggered grid system; first introduced by Harlow and Welch (1965). This grid distribution was used successfully in many codes and it is still the most prevalent grid arrangement. There are many advantages of this type of staggered grid arrangement. For a typical control volume, this discretized continuity equation contains the differences of adjacent velocity components. The discretized gradient of pressure in the momentum equation also contains adjacent pressure values. This arrangement prevents the occurrence of a wavy pressure and velocity fields in the numerical solutions. In the staggered

occurrence of a wavy pressure and velocity fields in the numerical solutions. In the staggered grid arrangement, the pressure difference between two adjacent grids becomes the driving force for the velocity component at the cell face between these grid points. Besides, the mass flow rate across each cell can be calculated without any interpolation for the relevant velocity component. The staggered arrangement of the grids also eliminated the need of specifying the pressure boundary conditions on the walls.

However, the staggered grid arrangement has its disadvantages too. In this arrangement, there are two distinct cells for the application of the finite analytic method to the two-dimensional momentum equation as shown in figure 3. This implies the need to evaluate two sets of finite analytic coefficients. In the three-dimensional problems three sets of coefficients must be evaluated for the momentum equations, one for each velocity component. This increases the CPU cost and memory requirement. The case of staggered grids also increases the difficulties in programming since different geometries parameters must be used for each grid.

To solve these problems Rhie and Chou (1983) introduced a non-staggered grid arrangement. In their method all variables are evaluated at the same location, the center of each control volume. The pressure gradient in the momentum equation is still evaluated by subtracting the pressures between two non-adjacent nodes. However, to compute the continuity equation, new velocity components on the volume faces are evaluated. These velocity components are obtained by an interpolation scheme based on the momentum equation. This method apparently devised by Rhie and Chow (1983) was further study by Miller and Schmidt (1988). They called it the pressure-weighted interpolation method (PWIM). They report that the PWIM scheme predicts physically unrealistic velocities in regions of rapidly varying pressure gradients.

The first successful application of a non-staggered grid arrangement to the finite analytic method was done by Aksoy (1989). Their method, called MWIM (Momentum Weighted Interpolation Method), is similar to the original Rhie and Chow (1983) PWIM method, but with a different interpolation scheme. The advantages and disadvantages of MWIM are similar to the PWIM method. There is only one set of FA coefficients to be evaluated for three-momentum equations, reducing memory and computational time. However, using this method, unrealistic velocity components are also obtained in regions of strong pressure gradient. This problem is specially severe in coarse grid calculations.

To overcome the problem mentioned above, for the staggered and non-staggered systems, a new scheme is used in the program FANS-3D. In this new scheme, a staggered grid system is used, but only one set of coefficients is evaluated. This method uses the staggered grid arrangement, but it also uses the main concepts of the MWIM and PWIM methods. The new scheme evaluates only one set of coefficients at the center of each control volume (see figure 4). The FA coefficients at the nodes of the velocity components are obtained by linear interpolation of the coefficients obtained at the centers of the control volumes. Details of this derivation are given by Bravo (1991). This method was fully tested and it is the method used in FANS-3D.

SOME APPLICATIONS OF THE PROGRAM

Conjugate Heat Transfer in Laminar Flow Between Parallel Conducting Plates (Extended Gratz Problem)

The geometry of the problem is represented in figure 5, where fully developed flow between two infinite parallel plates is moving from left to right. The domain has a total length of 10H with inlet height of H. The parallel plates have a thickness equal to 0.5H and are kept at constant temperature T_w on their external surfaces. The flow enters at uniform temperature T_f. The conductivities of the solid and fluid are k_s and k_f. The conductivity ratio $R_k = k_s/k_f$ determines the temperature in the solid fluid interface. If the conductivity ratio R_k is very high, the temperature on this interface is very close to the external surface temperature T_w. In this case, the problem is reduced to the original Gratz problem (Bravo, 1987). In general, the distribution of temperatures is determined by the peclet number Pe, and the conductivity ratio R_k.

The Gratz problem, when the temperature on the solid fluid interface is kept constant, was solved analytically by Prins, Mulder and Schenk (1949) and later numerically by Bravo (1987). The solution for the general conjugate heat transfer problem was later obtained by Mori, et.al.(1989). To solve the conjugate heat transfer problem, Mori et.al.(1989), represented the interfacial temperature distribution by infinite power series. They solved the governing energy equations for the solid and fluid domains using this temperature distribution as boundary condition. The Nusselt numbers, obtained by this procedure, were also presented in the form of infinite series. The major sources of error in their analysis are the truncation error during the evaluation of this infinite series and the simplification of the energy equation in the fluid flow domain. They assumed negligible diffusion in the longitudinal direction.

To compare with the results of Mori et.al. a Peclet number of 500 was selected. Four grid sizes of 10x3x9, 20x3x20, 40x3x40 and 80x3x80 along the x, y and z directions respectively were used. Insulated boundary conditions were applied on the solid inlet and outlet boundaries. The outlet boundary condition for the flow domain was considered fully developed or dT/dx = 0.0.

The dimensionless temperature, for this problem, is defined by

$$\theta = \frac{T - T_w}{T_f - T_w} \quad (3)$$

With this definition the dimensionless external surface temperature θ_w is equal to 0.0 and the dimensionless inlet temperature θ_f equal to 1.0. The local Nusselt number Nu_x is defined by

$$Nu_x = \frac{H\ q_f}{k_f(T_{fo} - T_m)} \quad (4)$$

where

q_f = heat flux at the solid fluid interface

T_{fo} = temperature at the solid-fluid interface

T_w = external constant surface temperature

T_f = uniform temperature of the incoming fluid

T_m = mixed mean temperature defined by $T_m = \frac{\int TUdA}{\int UdA}$

With $q_f = -k_f \frac{\partial T}{\partial n}$, and using the inlet height H as reference length, equation can be reduced to its dimensionless form

$$Nu_x = \frac{-1}{\theta_{fo} - \theta_{fm}} \frac{\partial \theta}{\partial n^*} \tag{5}$$

where $\theta_{fm} = \frac{\int \theta U dA}{\int U dA}$, θ_{fo} the dimensionless interface temperature and n^* the dimensionless normal.

The program FANS-3D finds the temperature θ at each nodal point. The Nusselt number is evaluated from this temperature distribution and equation (5).

Figure 6 compares the Nusselt number obtained by the program FANS-3D with the values obtained by Mori et. al. (1989) and discussed above. For the conductivity ratio $R_k = 1.0$, there is an excellent agreement between the results of Mori et. al. and the one provided by the program FANS-3D, for x values over 0.2. Below x = 0.2 the values given by Mori et. al. are under the ones given by the program FANS-3D. Theoretically, the Nusselt number at the entrance must go to infinity, which is correctly reproduced by the program. The lower values given by Mori et. al. are probably due to the simplified version of the energy equation used by them, which did not contain the diffusion term along the x direction. The Nusselt numbers for R_k equal to 100.0, 1000.0 and infinite are very close, indicating that for R_k over 100.0 the conjugate heat transfer problem behaves as the original Gratz problem. Theses values of the Nusselt number agree also quite well with the corresponding ones given by Mori et. al.(1989). They also coincide with the values computed by Bravo (1989) using the 9 point two-dimensional Finite Analytic method (these values are not shown in the figure). The program FANS-3D provides results that are reasonable and agree quite well with previous computations.

Conjugate Heat Transfer in a Compact Heat Exchanger

Another application example of FANS-3D is the compact heat exchanger shown in figure 7(a). This compact heat exchanger is similar to the class of compact heat exchangers known as offset-fin heat exchangers (Kays and London, 1984). To solve the complete compact heat exchanger is beyond the capacity of any computer, and a simplification is required. The flow between the finned plates is three-dimensional and very complex. The solution of the heat transfer problem is aggravated because of the conducting fins. The problem is a three-dimensional conjugate heat transfer problem. To obtain a solution to the problem we use the concept of fully developed flow extended to these geometries (Patankar, Liu and Sparrow, 1977). In this case, the velocity, a reduced pressure and a reduced temperature field become periodic after some entrance length. The reduced temperature is defined by

$$\theta(x,y,z) = \frac{T(x,y,z) - T_w}{T_{bx} - T_w} \tag{6}$$

where T_{bx} is the bulk temperature at any longitudinal position x. This situation is similar to the flow inside ducts of uniform cross section (Chapman, 1987). In this case, the shapes of the temperature profiles at successive streamwise locations separated by the periodic length L are assumed similar. Using this idea, it is possible to simplify the geometry of this problem and reduce the computational domain to the one represented in figures 7(b) and 7(c). An enlarged view of this small domain is shown in figure 8. The temperature in the front and back walls are

assumed constant and equal to Tw. The separation between the parallel plates is considered the reference length equal to L. The position of the fin and its dimensions are given in the same figure. The flow enters the domain in right hand side and leaves the domain in the left hand side, as shown by the arrows. The top and bottom surfaces are planes of symmetry.

Assuming constant properties, the temperature field and velocity fields are decoupled and their solution can be obtained independently. The governing equations for fluid flow are of the same type of the standard transport equation (1) and the program FANS-3D can be used without any modification.

To solve for temperature we define a new variable ϕ given by

$$\phi(x,y,z) = \frac{T(x,y,z) - T_w}{T_{bi} - T_w} \tag{7}$$

where T_{bi} is the inlet bulk temperature and T_w the external wall temperature. Using this definition and equation (6), the profiles of the dimensionless temperature at the ϕ_o at the outlet and ϕ_i at the inlet are of similar shape with the outlet condition being a constant times the inlet condition, or

$$\phi_o = \phi_i(\phi_{bo}) \tag{8}$$

where ϕ_{bo} is the bulk exit temperature. To determine the profiles of temperature at the inlet and outlet, an iterative procedure is required. We start assigning the temperature at the inlet $\phi_i(x,y) = \phi_{bi} = 1.0$, then the temperature on the outlet ϕ_o is obtained by solving the governing energy equation. Using the values of ϕ_o on the outlet the constant ϕ_{bo} is calculated by numerical integration at the outlet boundary. Finally, the temperature at the inlet ϕ_i is updated. This process is repeated until convergence is attained. All these steps are automatically performed by FANS-3D.

Figure 9 shows profiles of velocity component u along the y and z directions at the inlet and outlet planes, as obtained by the program FANS-3D. In this figure we can recognize the periodicity in the velocity distribution and the three-dimensional character of the flow. The flow not only moves up and down due to the presence of the beam, but also moves to the left and to right.

Figures 10(a) and 10(b) show the temperature profiles at three locations, at the inlet, on the beam and at the outlet. In these figures we can observe that the minimum dimensionless temperature ϕ is located on the lateral walls. The maximum temperatures are on the plane of symmetry. The temperature inside the fin, also shown in this figure, is almost constant in each cross section, but increases towards the center between the plates.

To study the effect of the fin, the pressure drop and the rate of heat transfer in this geometry can be compared with the ones for a fully developed flow between parallel plates. For example the pressure drop in the element of the heat exchanger, as computed by the program FANS-3D, is equal to -0.4565. For the equivalent situation, but without the fin the pressure drop is only -0.1200. Therefore, the increase in pressure drop due the fin is 280%.

The total increase in energy content, when the fluid moves from inlet to exit is given in Table 1. This table shows the energy increase in the element of heat exchanger for water and air and compares it with the one in a fully developed flow between parallel plates. The effect of the fin is an increase in the global rate of heat transfer of 68.7% for water and 54.2% for air. An additional computation with an infinite conductivity of the solid showed a less than 0.2% change in the rate of heat transfer. Thus, to improve the design of the compact heat exchanger, it is

possible to reduce the thickness of the fin without significantly affecting the rate of heat transfer, but reducing the pressure drop. Furthermore, the analysis in the temperature distribution shows that an staggered distribution of fins can be more effective than the regular one.

Conjugate Heat Transfer in Electronic Modules

In this section, the combined effect of convection, and radiation heat transfer is studied in an array of electronic chips displayed in figure 11. The chips are cooled by a radiatively non-participating gas flowing inside the passage. The program FANS-3D and the subroutine ANDISOR4 (Sanchez, Smith & Krajewski, 1990) were used to study the problem. The three-dimensional convection part of the problem was solved using the 19-point Finite Analytic Method and the radiation analysis using the discrete ordinates method (Sanchez, Smith & Krajewski, 1990). Results showing the effects of convection alone, combined radiation and convection, and the presence or not of a radiatively participating medium are presented.

To simplify the solution fully developed periodic flow is assumed (see discussion for the previous problem). Using this concept of periodicity along the x direction and considering some of the planes of symmetry, the problem can be reduced to the element represented in figures 11(b) and 11(c). The dimensions in centimeters of this element are given in figure 12. The fluid flow is in the positive x direction. The planes at y=0.0 and at y=1.5 are considered planes of symmetry; and the top and bottom walls are adiabatic. The inlet temperature of the fluid is considered equal to 305 K and the temperature of the blocks constant and equal to 320 K. All surfaces are assumed black. The fluid is considered radiatively non-participating transparent gas (air) with constant properties. The flow is considered laminar.

The Navier-Stokes equations are decoupled from the energy equation and the fluid field can be solved independently. The solution was obtained using the program FANS-3D with the 19-point Finite Analytic method. Once this solution was performed, the energy equation was solved using the same method explained above for the compact heat exchanger. The coupling between radiation and convection is done through energy balances on the walls. The existing radiative transfer code, ANDISORD4 (Sanchez, Smith & Krajewski, 1990), was used to solve for radiation. An S-8 implementation (80 discrete directions) of the discrete-ordinates model is applied. Although not required, the grids for the flow and radiation models are identical. When the medium is non-participating, the divergence of the radiative heat flux vector vanishes, and the transport and radiation model become explicitly decoupled. Implicitly, however, the two models are interdependent through the temperature field and the wall heat fluxes.

The results for the flow field computation are shown in figures 13 through 14. The velocity profiles for the u component are shown in figure 13 at two locations, at the inlet and the center between the blocks. From these figure, we can appreciate that the velocity between the blocks and the upper plate is similar to the velocity between two plates, or Poiseuille flow. For Reynolds number of 100 the velocities between the blocks are quite small. Figure 14 displays velocity vectors on the back plane of symmetry. In this last figure, at the center of the blocks, the flow is rotating counterclockwise. Figure 15 show velocity vectors on a plane located between the blocks in the x direction. This figure shows that some fluid is entrained from the top of the blocks and is transported to the lower sides.

Profiles of dimensionless temperature ϕ on three different planes are shown in figures 16 and 17. The temperature of the blocks is zero and the bulk inlet temperature is equal to one. Figure 16 shows these profiles when convection heat transfer alone is considered. As we expect

the profiles are perpendicular to the top and bottom insulated plates. In this figure we can also appreciate that the fluid moving between the blocks has a temperature very close to the temperature of the blocks. Specifically, the fluid near the bottom wall has almost the same temperature of the blocks. The maximum dimensionless temperature (coldest dimensional temperature) is on the top insulated wall.

Figure 17 shows dimensionless temperature profiles when convection and radiation are included. The temperature profiles are quite different from the ones discussed in figure 16. The maximum value of the temperature is in the center region between the top plate and the blocks. The top and bottom plates have an intermediate temperature between the temperature of the blocks and the temperature in the center region. The higher temperature of the top plate and the lower temperature on the bottom plate, compared with the convection case alone shown in figures 16, is because of the radiation effect. The top plate receives a net radiation coming from the blocks and the bottom plate. Because this plate is insulated, this arriving net radiant energy is dissipated by convection, which is indicated by a positive slop of the profile at this point. The ϕ profile has a maximum in the center region and decreases as we move closer the bottom plate. However, close to the bottom plate this profile increases again. This increase indicates that heat is transfer by convection from the fluid to the bottom wall. Because this wall is insulated, the same amount of energy is irradiated to the top wall.

An energy balance when convection-radiation heat transfer was considered shows an increase on the rate of heat transfer of 49.1% compared with the computation considering only convection heat transfer. In this problem then radiation is a very important and must be considered.

This final problem of electronic modules is an example of a three-dimensional conduction-convection-radiation heat transfer problem. Although conduction was not explicitly discussed, the problem was solved assuming infinite (10^{30}) conductivity in the blocks. In this situation the blocks assume a constant temperature everywhere resembling an isothermal body. The convection and convection-radiation results show the potential of the program FANS-3D in the simulation of complex three-dimensional problems that include all modes of heat transfer.

CONCLUSIONS

This study shows the solution of complex three-dimensional problems that included conduction convection and radiation modes of heat transfers with the application of the program FANS-3D. The study of these problems also shows different types of boundary conditions from the simplest boundary when the values of the variable are assigned on the boundary, to symmetric and periodic boundaries. The solutions were presented in the form of vectors and profiles given by the graphics part of the program FANS-3D. This graphic program also displays contours that include shading. The difficulties in reproducing these colors do not allow the inclusion of these pictures in this work.

Table 1 Comparison Between Energy Increase in the Element of Heat Exchanger and Energy Increase in Flow Between Parallel Plates

	Water	Air
Pr	1.76	0.704
k(W/m°C)	0.6775	31.27×10^{-3}
$\Delta E_{\text{with fin}}/C_1$	0.07075	0.15658
$\Delta E_{\text{parallel plates}}/C_1$	0.04194	0.10157
Inc. %	68.7	54.2

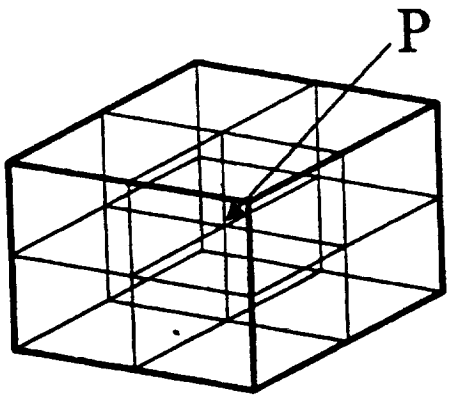

Figure 1 Finite Analytic Element

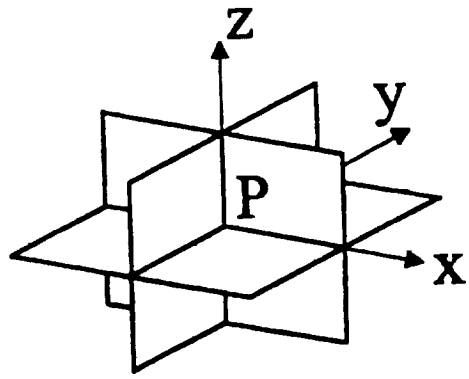

Figure 2 19-point FA Method

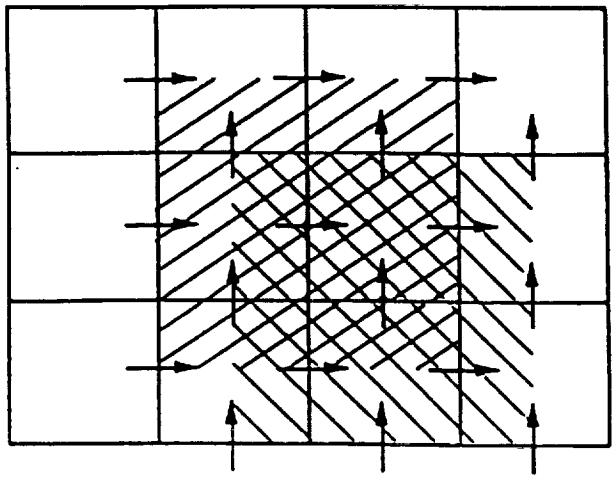

Figure 3 FA Cells in a Staggered Arrangement

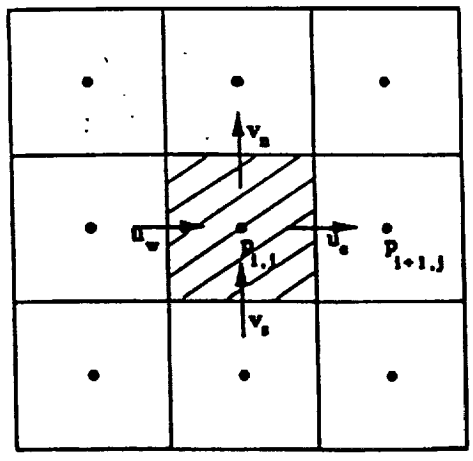

Figure 4 Evaluation of FA Coefficients in the New Method

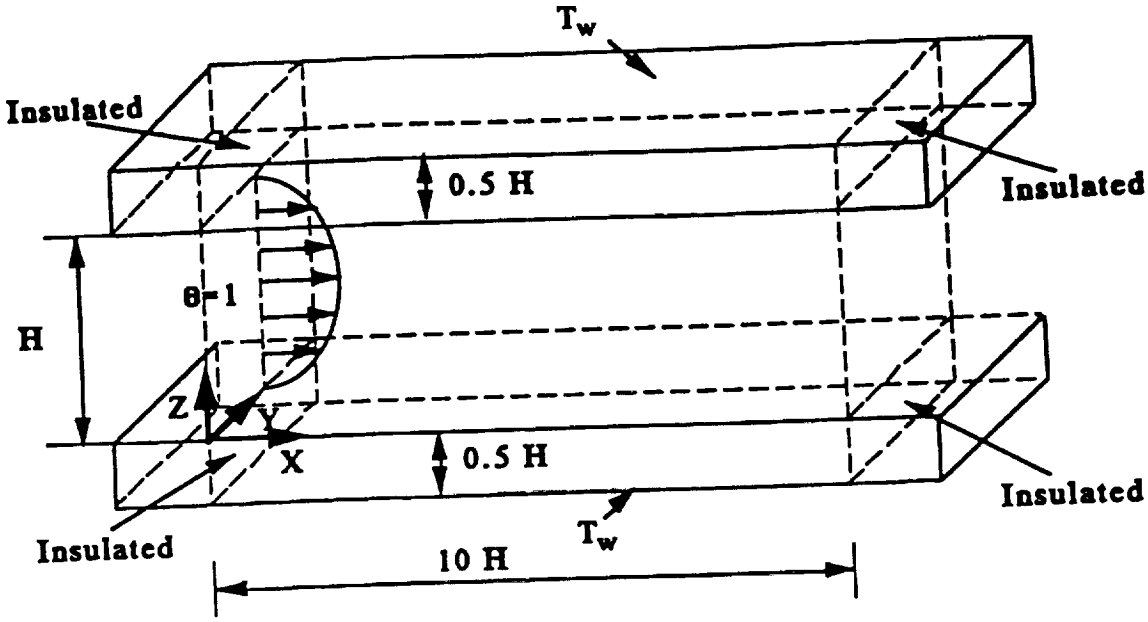

Figure 5 Domain of Solution for the Extended Gratz Problem

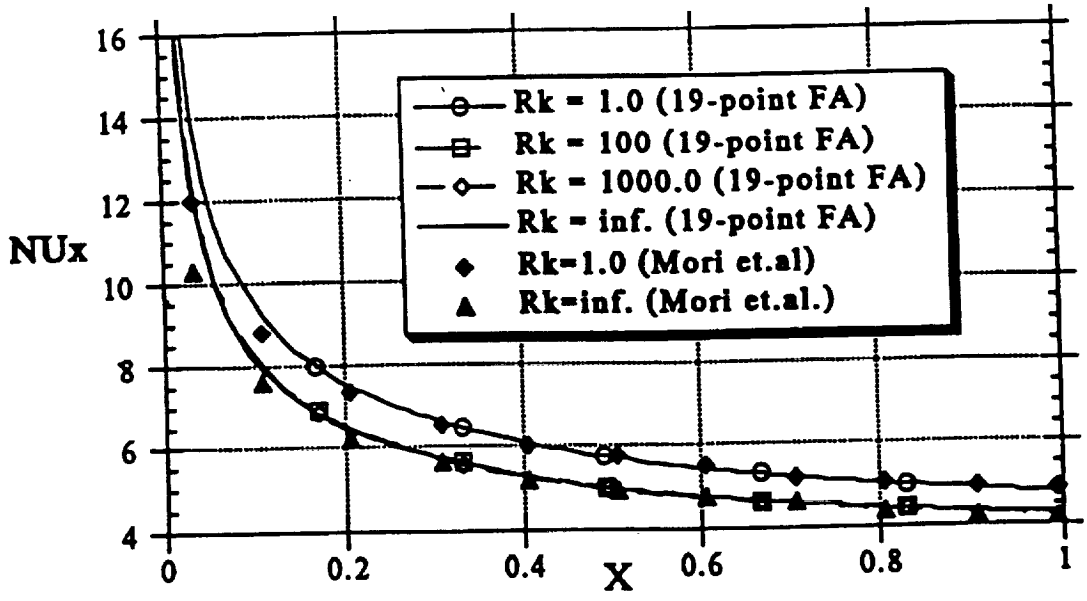

Figure 6 Local Nusselt Number at Different Locations

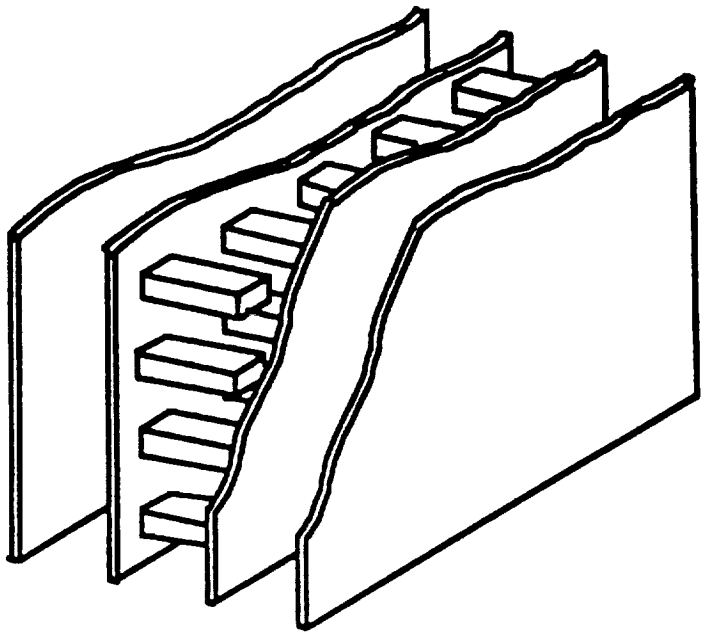

(a)

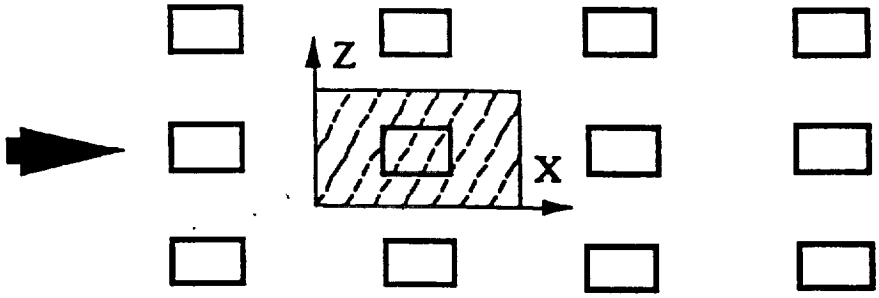

(b)

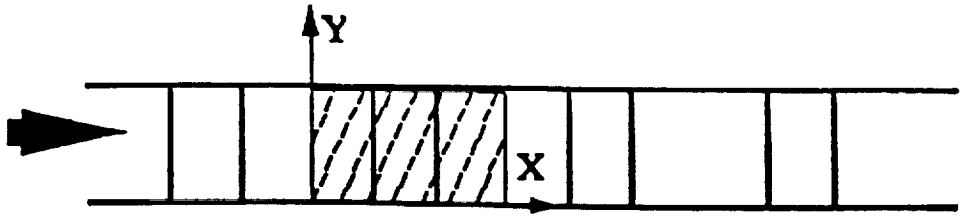

(c)

Figure 7 Heat Transfer Analysis in a Compact Heat Exchanger

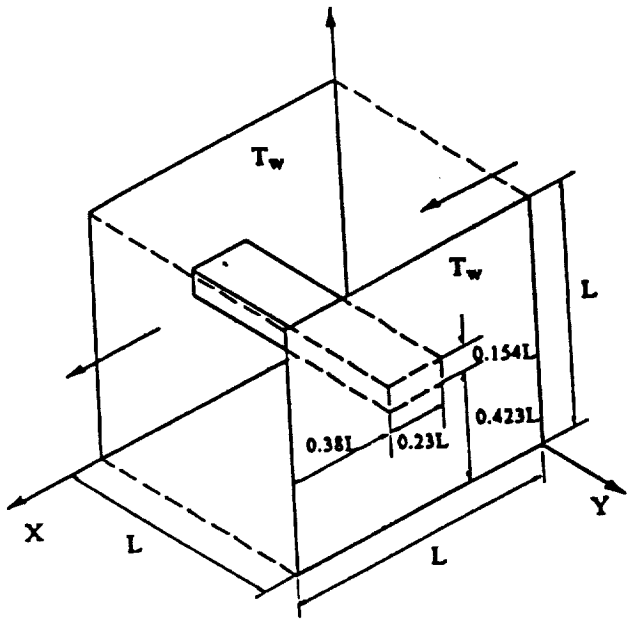

Figure 8 3-D View of the Element Shown in Figures 7 (b) and (c) of a Compact Heat Exchanger

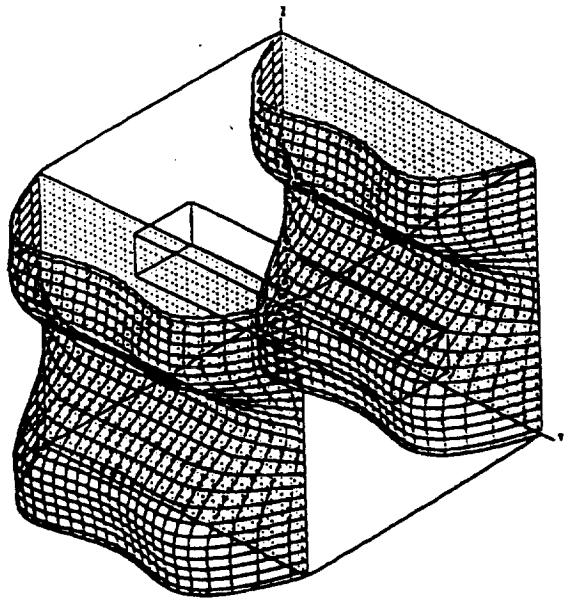

Figure 9 Profiles of U Velocity Component on the Inlet and Exit Planes. 3-D View

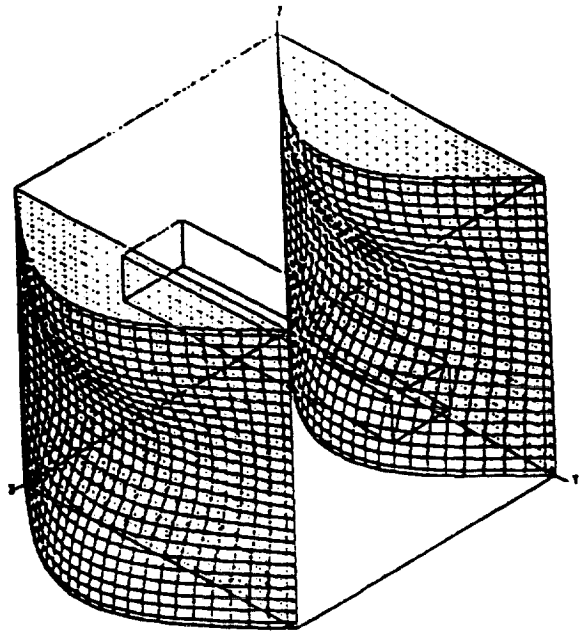

(a)

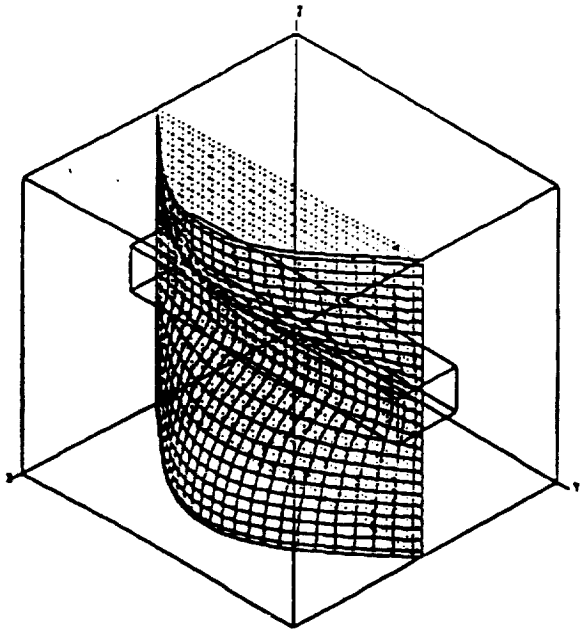

(b)

Figure 10 Temperature Profiles on Three Different Planes

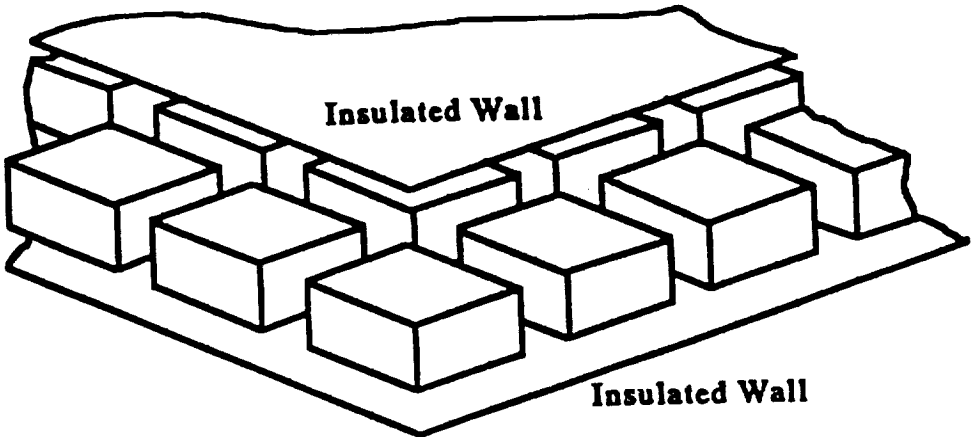

(a)

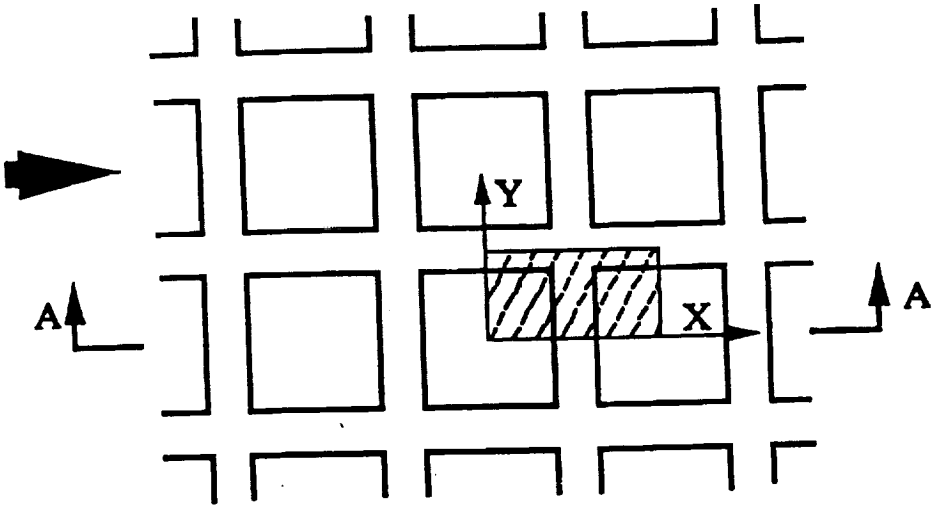

(b)

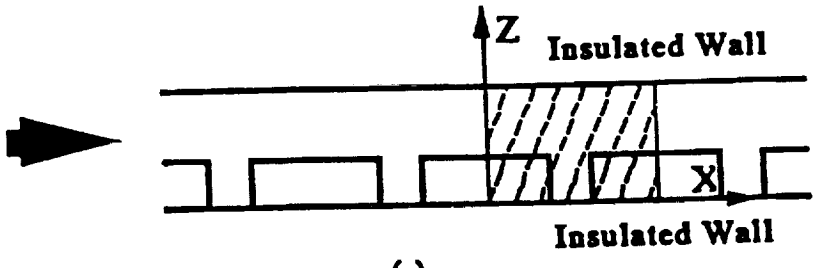

(c)

Figure 11 Heat Transfer Analysis of Electronic Components

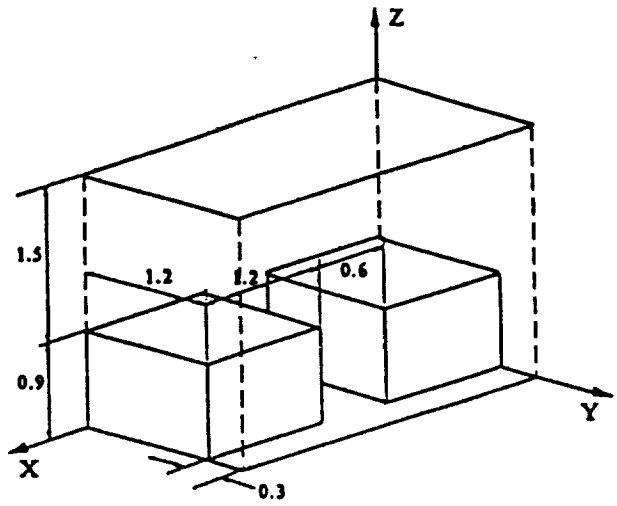

Figure 12 Domain of Solution of the Electronic Components Shown in Figure 11

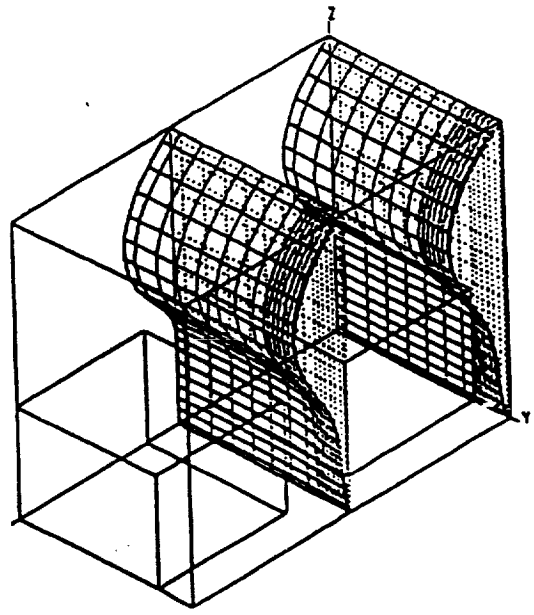

Figure 13 Profiles of Velocity Components U 3-D View

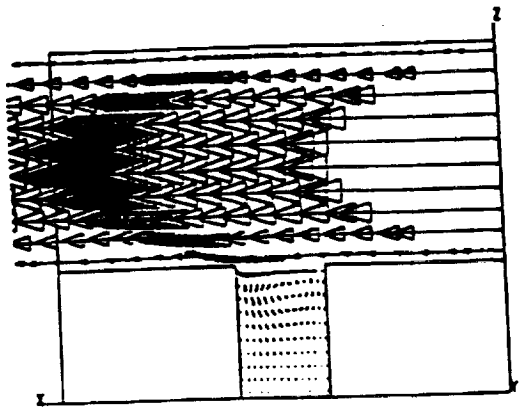

Figure 14 Velocity Vectors on Plane of Symmetry y = 0

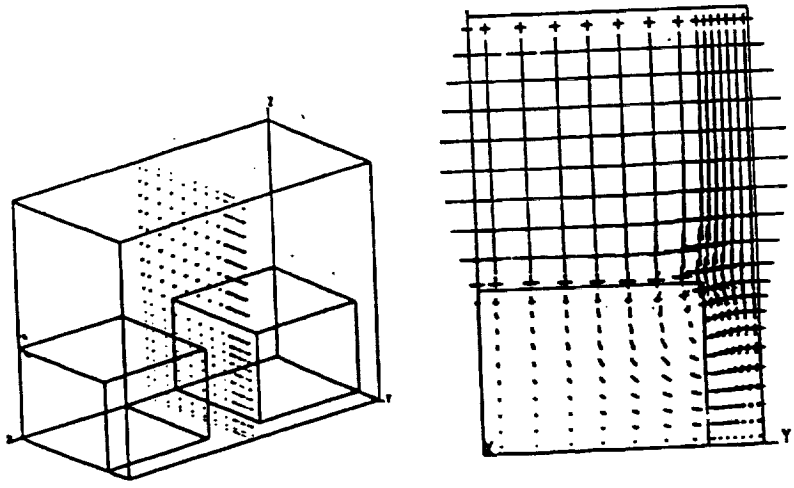

Figure 15 Velocity Vectors on Plane x = 1.5

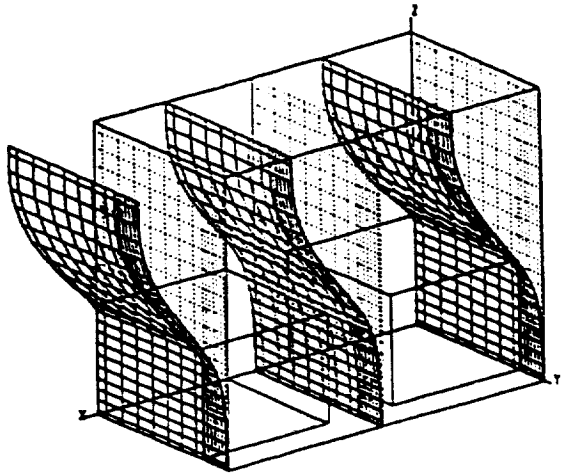

Figure 16 Dimensionless Temperature Profiles
Conduction-Convection Problem

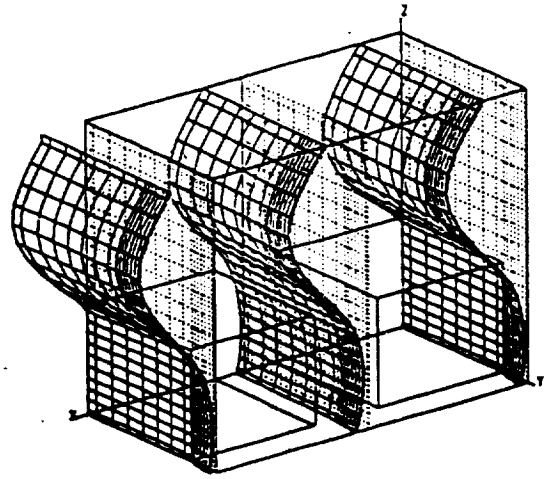

Figure 17 Dimensionless Temperature Profiles
Conduction-Convection-Radiation Problem

REFERENCES

Aksoy H., (1989), "Finite analytic numerical solution of fluid flow and heat transfer with non-staggered grids," Master Thesis. The University of Iowa. Iowa City. Iowa.

Bravo, R. H., (1987), "Computer-aided analysis of two-dimensional fluid flow and convective heat transfer," Master Thesis. The University of Iowa. Iowa City. Iowa.

Bravo, R. H., (1991), "Development of the three-dimensional finite analytic method for simulation of fluid flow and conjugate heat transfer,"Ph.D. Thesis. The University of Iowa. Iowa City. Iowa.

Chapman, A. J., (1987), "Fundamentals of heat transfer," Macmillan Publishing Co. New York.

Harlow, F. H. and Welch, J. E., (1965), "Numerical calculation of time-dependent viscous incompressible flow of fluid with free surface," Phys. Fluids, Vol. 8, No. 12, pp. 2182-2189.

Issa, R. I., Gosman, A. D. and Watkins, A. P., (1986), "The computation of compressible and incompressible recirculating flows by a non-iterative implicit scheme," J. of Computational Physics, Vol. 62, pp. 66-82.

Kays, W. M. and London, A. L., (1984), "Compact heat exchangers," McGraw-Hill Co. New York, Third edition.

Miller, T. F. and Schmidt, F. M., (1988), "Use of a pressure-weighted interpolation method for the solution of the incompressible Navier-Stokes equations on a nonstaggered grid system," Numerical Heat Transfer, Vol. 14, pp. 213-233.

Mori, S., Shinke, T., Sakakibara, M. and Tanimoto, A. (1979), "Steady heat transfer to laminar flow between parallel plates with conduction in wall," Kagaku Kogaku Ronbunshu, 1, pp. 235-240.

Patankar, S. V. (1980), "Numerical heat transfer and fluid flow," McGraw-Hill Co. New York.

Patankar, S. V. and Spalding, D. B. (1972), "A calculation procedure for heat, mass and momentum transfer in three-dimensional parabolic flows," Int. J. Heat Mass Transfer, Vol. 15, pp. 1787-1806.

Patankar, S. V., Liu, C. H. and Sparrow, E. M. (1977), "Fully developed flow and heat transfer in ducts having streamwise-periodic variations of cross-sectional area," J. Heat Transfer, Vol. 99, pp. 180-186.

Prins, J. A., Mulder, J. and Shenk, J. (1949), "Heat transfer in laminar flow between parallel plates," Applied Scientific Research, Vol 1-2, Sec. A, pp. 431-439.

Rhie, C. M. and Chow, W. L. (1983), "Numerical study of the turbulent flow past an airfoil with trailing edge separation, " AIAA., Vol. 21, pp. 1525-1532.

Sanchez, A. , Krajeswski, W. and Smith, T. F., (1990), "Statistical framework for validation of satellite-based global precipitation simulation; Part I: An atmospheric radiation model - The plane layer case," Porgress report prepared for Grant NA89AA-D-AC195 for National Oceanic and Atmos. Admin.

Van Doormal, J. P. and Raithby,G.D.,(1984), "Enhancements of the SIMPLE method for predicting incompressible fluid flows," Numerical Heat Transfer, Vol. 7, pp.147-163.